Bosonization and entanglement spectrum for one-dimensional polar bosons on disordered lattices

2013 New J. Phys. 15 045023

(http://iopscience.iop.org/1367-2630/15/4/045023)

New Journal of Physics
The open access journal for physics

Bosonization and entanglement spectrum for one-dimensional polar bosons on disordered lattices

Xiaolong Deng[1,5], Roberta Citro[2], Edmond Orignac[3], Anna Minguzzi[4] and Luis Santos[1]

[1] Institut für Theoretische Physik, Leibniz Universität Hannover, Appelstraße 2, D-30167 Hannover, Germany
[2] Dipartimento di Fisica 'E R Caianiello' and Spin-CNR, Università degli Studi di Salerno, Salerno, Italy
[3] Laboratoire de Physique de l'École Normale Supérieure de Lyon, CNRS-UMR5672, F-69364 Lyon Cedex 7, France
[4] Université Grenoble-Alpes and CNRS, Laboratoire de Physique et Modélisation des Milieux Condensés UMR 5493, Maison des Magistères, BP 166, F-38042 Grenoble, France
E-mail: Xiaolong.Deng@itp.uni-hannover.de

New Journal of Physics **15** (2013) 045023 (12pp)
Received 1 February 2013
Published 26 April 2013
Online at http://www.njp.org/
doi:10.1088/1367-2630/15/4/045023

Abstract. Ultra cold polar bosons in a disordered lattice potential, described by the extended Bose–Hubbard model, display a rich phase diagram. In the case of uniform random disorder one finds two insulating quantum phases—the Mott-insulator and the Haldane insulator—in addition to a superfluid and a Bose glass phase. In the case of a quasiperiodic potential, further phases are found, e.g. the incommensurate density wave, adiabatically connected to the Haldane insulator. For the case of weak random disorder we determine the phase boundaries using a perturbative bosonization approach. We then calculate the entanglement spectrum for both types of disorder, showing that it provides a good indication of the various phases.

[5] Author to whom any correspondence should be addressed.

Contents

1. Introduction

The extraordinary experimental advances on the realization and control of ultracold quantum gases subjected to optical lattice potentials [1] pave the way for the application of these systems as 'quantum simulators' [2], capable of exploring with unprecedented accuracy complex models from condensed matter physics [3, 4] to high-energy physics [5].

The investigation of the interplay of disorder and interaction effects remains an open question in condensed matter physics, linked to the study of the metal–insulator transition. For bosonic systems, the Bose glass phase [6, 7] is an example of a novel strongly correlated phase arising from the simultaneous effect of disorder and interactions. Most solid-state based physical systems have to deal with some amount of disorder, which originates e.g. from defects in the material or impurity atoms. A very peculiar feature of quantum gases is that one can add a tunable and controllable amount of disorder in the pure system. In the regime of vanishing interactions, Anderson localization has been observed, first in one spatial dimension [8, 9] and then also in three dimensions [10, 11]. The Bose glass phase (BG) has also been explored with bosons with short-range interactions on a lattice [12].

The very recent advances on trapping and cooling ultracold molecules [13] and atoms with a large dipole moment [14, 15] lead to the exploration with atomic quantum simulators of yet another set of systems, those with long-range interactions. For the case of one-dimensional bosons on a lattice, the minimal model accounting for longer-range interactions is the extended Bose–Hubbard model, which includes next-neighbour interactions among the bosons. In the case of a clean system, the extended Bose–Hubbard model already displays a rich phase diagram which, in addition to the Mott insulator (MI) already found in the Bose–Hubbard model [7], features several novel insulating phases, i.e. the density wave (DW) and the Haldane insulator (HI) [16, 17]. The DW phase is characterized by a spatial modulation of the density profile, i.e. it displays quasi-long-range diagonal (or crystal) order, while the HI is characterized by a non-local order parameter (hidden or string order, defined in section 2.2 below). At average unitary lattice filling, the HI density profile features a regular sequence of spatial modulations with on-site filling either 0 or 2, diluted in an arbitrary sequence of sites with filling 1 [17].

In this context, a relevant question arises regarding the fate of such insulating phases under the effect of disorder, as well as which novel phases arise in the presence of disorder.

In the strong-coupling regime and for unitary lattice filling, a good starting point to understand this behaviour is to map the problem onto spin chains. For the latter system, the stability of the various insulating phases at weak disorder has been studied using renormalization group arguments [18–24] and numerical methods [25–28]. For example, the DW phase is found to disappear at infinitesimally small disorder, according to the Imry–Ma argument [29, 30]. In analogy to the results known for the Bose–Hubbard model, other insulating phases are expected to shrink in the phase diagram, in favour of disordered correlated phases of the Bose-glass type. The mapping onto spin systems fails when the tunnel energy becomes sufficiently important with respect to repulsive interactions to allow large occupancy of given lattice sites, and a superfluid (SF), gapless phase builds up. In the general case, the problem has to be addressed numerically, and we have recently explored it using density-matrix renormalization group (DMRG) method [31], establishing a phase diagram by following the behaviour of several correlation functions.

In this work, we support the phase diagram using two complementary tools: a bosonization and renormalization group description at weak disorder, and the study of the entanglement spectrum for the system. The bosonization approach combined with perturbative renormalization group methods allows us to provide relevant information on the phase diagram in the weak disorder region. It predicts that the qualitative shape of the phase diagram close to the MI–HI transition depends on the value of the on-site interactions. We perform DMRG simulations for two values of the on-site interactions to check this picture. The entanglement spectrum allows us to obtain the phase diagram by an alternative approach to the study of correlation functions. It is based on the fact that the largest eigenvalues of the reduced density matrix of a sub-system carry information on the phase of the system. We show that this recently developed approach turns out to be useful to recognize the various phases of disordered lattice bosons.

2. The model, numerical methods and phase diagrams

We consider a system of N dipolar bosons confined onto a one-dimensional deep optical lattice and in the presence of a very shallow trapping potential. We assume the dipole orientation to be perpendicular to the lattice direction and truncate the dipole–dipole interaction potential to nearest-neighbour (NN) interactions. Although longer range interactions do play a role, for very weak interactions and sufficiently large dipoles, the most relevant properties of dipolar physics can already be understood from a model of bosons with NN interactions, which will be denoted 'polar bosons' for short. This leads to the Hamiltonian of the extended Bose–Hubbard model

$$H = -t \sum_i (b_i^\dagger b_{i+1} + \text{h.c.}) + \frac{U}{2} \sum_{i=1}^{N} n_i(n_i - 1) + V \sum_i n_i n_{i+1} + \sum_i \epsilon_i n_i, \qquad (1)$$

where $b_i^\dagger$, b_i are creation and annihilation operators for bosons at site i, $n_i = b_i^\dagger b_i$ are the number operators, t is the tunnel energy and $U(V)$ are the on-site NN interaction energies. Disorder is included in the model either through the random on-site energies ϵ_i, chosen to be uniformly distributed in the interval $[-\Delta, \Delta]$, or by a quasiperiodic potential $\epsilon_i = \Delta \cos(2\pi\alpha i + \phi)$, with $\alpha = (\sqrt{5} - 1)/2$ characterizing the incommensurability of the secondary lattice. The system length is chosen according to the Fibonacci series $L = 55, 89, 144, 233$ in order to make the system as close as possible to a periodic one.

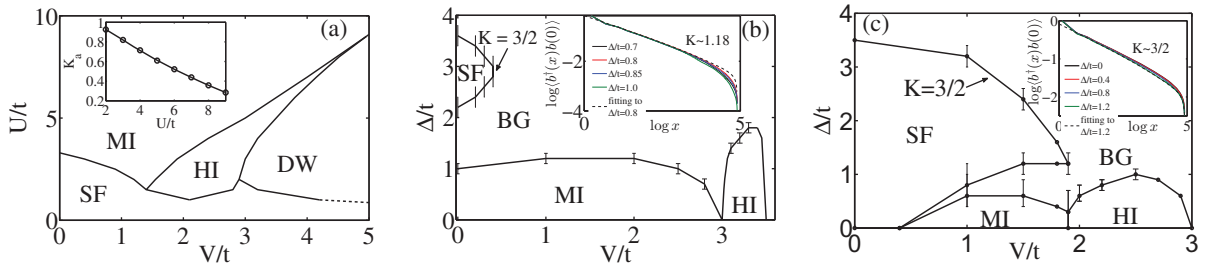

Figure 1. Phase diagram for polar bosons with NN interactions. Left panel: clean case in the plane $(V/t, U/t)$, with inset showing the value of the Luttinger parameter K_a along the MI–HI critical line, which is described by a Luttinger model. The HI–DW critical line belongs to the Ising universality class [42]. Central and right panel: case of uniform disorder, in the plane $(V/t, \Delta/t)$ for $U/t = 5$ and $U/t = 3$. The insets show the DMRG results (solid lines) for the one-body correlator $\langle b^\dagger(x)b(0)\rangle$ at increasing disorder and at fixed $V/t = 2.9$ in (b) and $V/t = 1.9$ in (c), close to the MI–HI transition point. At the transition to the Bose-glass phase, the best fit with the finite-size power-law expression [43] no longer matches the data, as illustrated by the dashed line.

2.1. Numerical method

We have studied the extended Bose–Hubbard model using the DMRG method with open boundary conditions [32–36]. The considered system sizes range up to 233 sites and we have taken up to 60 disorder realizations per point. In order to avoid the presence of metastable states we allow the number of optimal states to shrink or expand at every DMRG step according to a two-step algorithm. The algorithm keeps at least one of the eigenvectors in the blocks of the reduced density matrix[6] if they have only zero eigenvalues, and then keeps an additional eigenvector with zero eigenvalue in the block with non-zero eigenvalues if they decay very sharply to zero. The number of sweeps in the DMRG is 12 for weak disorder and up to 20 for strong disorder. Furthermore, we have eliminated the edge states in the HI phase by adding one more particle or by coupling two extra hard-core bosons at the edges of the chain in order to form a singlet state [37].

2.2. Phase diagram of the extended Bose–Hubbard model without disorder

The phase diagram of the extended Bose–Hubbard model in the absence of disorder is known [16, 17] and is illustrated in figure 1. If the tunnel energy is dominating on the on-site interactions the bosons are delocalized throughout the lattice and the system is SF. The fluid displays quasi-long-range order, with an algebraic decay of the first-order correlation function $G(r) = \langle b_i^\dagger b_{i+r}\rangle / \sqrt{\langle n_i\rangle\langle n_{i+r}\rangle} \propto r^{-1/2K}$. At increasing on-site interactions and weak NN interactions a Kosterlitz–Thouless transition occurs towards the incompressible MI phase, characterized by a hidden parity order $\mathcal{O}_P = \lim_{|i-j|\to\infty}\langle(-1)^{\sum_{i<l<j}\delta n_l}\rangle$ [17], where $\delta n_l = 1 - n_l$. At sufficiently large values of U and intermediate values of V a second insulating phase is found. This HI is characterized by a hidden string order [17] $\mathcal{O}_S = \lim_{|i-j|\to\infty}\langle\delta n_i(-1)^{\sum_{i<l<j}\delta n_l}\delta n_j\rangle$,

[6] As usual in DMRG, the reduced density matrix is made block-diagonal with respect to the number of particles.

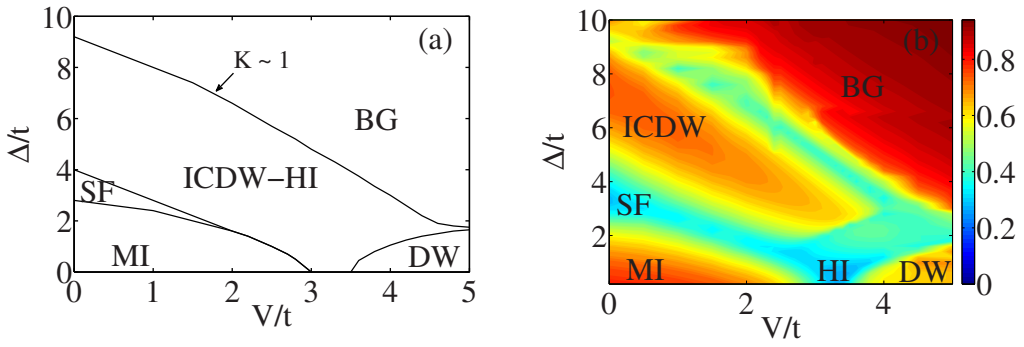

Figure 2. Phase diagram for polar bosons with NN interactions in a quasiperiodic potential in the plane $(V/t, \Delta/t)$ for $U/t = 5$. Left panel: phase diagram from the study of correlations functions as in [31]. Right panel: results from the entanglement spectrum function ζ as defined in the text, for a system of size $L = 89$.

associated with the breaking of the $Z_2 \times Z_2$ symmetry, and equivalent to a 'valence-bond' solid [38] picture of the HI for spin systems. At sufficiently large values of V and U a third insulating phase occurs, a DW with spatial modulation as can be identified by the finite correlator $\mathcal{O}_{\mathrm{DW}} = \lim_{|\mathrm{i}-j|\to\infty}\langle(-1)^{\mathrm{i}-j}\delta n_i \delta n_j\rangle$. At sufficiently large U a direct first-order transition is expected between MI and DW.

2.3. Phase diagram of the disordered extended Bose–Hubbard model

The phase diagram of the extended Bose–Hubbard model in presence of uniform disorder has been first studied in [31] by the study of correlation functions and gaps, and is illustrated in figure 1. Among the phases of the pure system, the DW phase is unstable under infinitesimal disorder according to the Imry–Ma argument [29], and thus disappears. The MI and HI disappear at sufficiently strong disorder to leave a compressible, non-superfluid Bose-glass phase [6, 7, 39]. An additional SF lobe is found at finite disorder as observed in [40, 41] for $V = 0$, and corresponds to the regime where repulsions overcome localization effects [6].

It is not easy to resolve numerically the behaviour of the critical MI–HI point for weak disorder, and in particular whether the critical line remains stable or whether a Bose glass intermediate region opens at $\Delta = 0$. To draw the phase diagram in this regime we use input from bosonization and renormalization arguments (see section 3 below).

2.4. Phase diagram of the extended Bose–Hubbard model with quasiperiodic potential

For the case of a quasiperiodic potential the phase diagram (shown in figure 2) considerably differs from the one with uniform disorder [31]. The main features are the presence of an incommensurate density wave phase (ICDW), typical of the quasiperiodic potentials [44, 45], adiabatically connected to the HI phase, and the persistence of a DW phase, due to the intrinsically different nature of the quasiperiodic potential with respect to a truly random potential [46].

3. Bosonization approach at weak disorder

For sufficiently strong interactions, where number fluctuations on each site are relatively small, we truncate the occupancy of each site to the values $\{0, 1, 2\}$. We then employ the Holstein–Primakoff transformation $S_i^z = \delta n_i = 1 - n_i$, $S_i^+ = \sqrt{2 - n_i} b_i$ to map the extended Bose–Hubbard model onto a spin-1 Hamiltonian with single-ion anisotropy:

$$H = -2t \sum_i S_i^x S_{i+1}^x + S_i^y S_{i+1}^y + V \sum_i S_i^z S_{i+1}^z + U/2 \sum_i (S_i^z)^2. \tag{2}$$

Following the early works of Timonen and Luther [47] and Schulz [48] we represent the spin-1 operators as the sum of two spin-1/2 operators, $S_i^\alpha = \sigma_{i,1}^\alpha + \sigma_{i,2}^\alpha$. This brings the Hamiltonian (2) into the one of two coupled spin chains. Furthermore, a Jordan–Wigner transformation is employed to map the spin-1/2 operators onto fermions according to $\sigma_{i,\lambda}^z = a_{i,\lambda}^\dagger a_{i\lambda} - 1/2$, $\sigma_{i,\lambda}^+ = a_{i,\lambda}^\dagger e^{i\pi \sum_{n=1}^{i-1} a_{n,\lambda}^\dagger a_{n,\lambda}}$, with $\lambda = 1, 2$. A continuum limit $a_{n,\lambda} = \sqrt{a} \sum_{p=\pm} \psi_p^\lambda(na)$ where a is the lattice spacing and p stands for $\pm$, depending on whether a left or right mover is taken. Finally, one employs a low-energy description of each fermionic field, $\psi_p^\lambda(x) \sim \frac{1}{2\pi\alpha} e^{ipk_F x} e^{-i(p\phi_\lambda(x) - \theta_\lambda(x))}$, where the fields $\theta_\lambda(x)$ and $\phi_\lambda(x)$ satisfy the canonical commutation relations $[\phi_\lambda(x), \partial_x \theta_{\lambda'}(x')] = i\pi \delta_{\lambda\lambda'} \delta(x - x')$. We have $k_F = \pi/(2a)$ when $\langle S^z \rangle = 0$, i.e. the filling is one boson per site. This leads to the Hamiltonian of two coupled Tomonaga–Luttinger fluids [22, 48, 53], which takes a simple form $H = H_a + H_o$ once the 'acoustical' and 'optical' combinations are introduced $\phi_a = (\phi_1 + \phi_2)/\sqrt{2}$, $\phi_o = (\phi_1 - \phi_2)/\sqrt{2}$, and similarly for the θ_λ fields,

$$H_a = \frac{\hbar u_a}{2\pi} \int dx \left[K_a (\partial_x \theta_a)^2 + \frac{1}{K_a} (\partial_x \phi_a)^2 \right] + \frac{g_1}{(\pi a)^2} \int dx \cos(\sqrt{8}\phi_a), \tag{3}$$

$$H_o = \frac{\hbar u_o}{2\pi} \int dx \left[K_o (\partial_x \theta_o)^2 + \frac{1}{K_o} (\partial_x \phi_o)^2 \right] + \frac{g_2}{(\pi a)^2} \int dx \cos(\sqrt{8}\phi_o) + \frac{g_3}{(\pi \alpha)^2} \int dx \cos(\sqrt{2}\theta_o), \tag{4}$$

where $g_1 = g_2 = (U - V)a$ and $g_3 = -2ta$. Coupling between acoustical and optical sectors is found at a higher order [16, 17] and is therefore less relevant than the terms listed here. The weak-coupling expressions for the Luttinger parameters entering equations (3) and (4) read

$$u_a = 2ta \sqrt{1 + \frac{U + 6V}{2\pi ta}}, \qquad K_a = \frac{1}{\sqrt{1 + \frac{U+6V}{2\pi ta}}}, \tag{5}$$

$$u_o = 2ta \sqrt{1 - \frac{U - V}{2\pi ta}}, \qquad K_o = \frac{1}{\sqrt{1 - \frac{U-V}{2\pi ta}}}. \tag{6}$$

Introducing the re-scaled fields $\theta_{+/-} = \theta_{a/o}/\sqrt{2}$ and $\phi_{+/-} = \sqrt{2}\phi_{a/o}$, the Hamiltonians in equations (3) and (4) can be brought to the form used in [16, 17].

The phase diagram [48] can be deduced from (3) and (4). For $K_a > 1$ in (3), the cosine term is irrelevant, and the 'acoustic' modes are gapless. For $K_a < 1$ the cosine term is relevant, and the field ϕ_a is pinned either to 0 for $g_1 < 0$ or to $\pi/\sqrt{8}$ for $g_1 > 0$, the spectrum of H_a being always gapped. Meanwhile in (4), at least one of the two cosines is relevant therefore the spectrum

is always gapful. Depending on the parameters, either θ_o or ϕ_o is pinned. When ϕ_o (resp. θ_o) is pinned, the correlation functions of its dual fields $e^{i\beta\theta_o}$ (resp. $e^{i\beta\phi_o}$) decay exponentially. Combining the different possibilities we obtain the two gapless SF phases (when $K_a > 1$ and either ϕ_o or θ_o is pinned), the gapful DW phase (when both ϕ_a and ϕ_o are pinned), and two phases with ϕ_a pinned and θ_o pinned. The phase with ϕ_a pinned to zero (i.e. $g_1 < 0$) is the MI, while the phase with ϕ_a pinned to $\pi/\sqrt{8}$ (i.e. $g_1 > 0$) is the HI [16, 17].

In the following we focus on the parameter regime corresponding to the HI–MI transition point at weak disorder. This regime is difficult to access numerically, but is amenable to a perturbative renormalization group calculation. At the critical point $g_1 = 0$ which separates the Mott-insulating from the Haldane insulating phase, the system is in a Luttinger liquid state [49–52] and the boson Green's function decays as

$$\langle b^\dagger(x)b(0)\rangle = |C|^2 \left(\frac{\alpha}{|x|}\right)^{\frac{1}{4K_a}}. \tag{7}$$

One kind of randomness that we are able to treat is the on-site disorder of the form $\sum_n \epsilon_n b_n^\dagger b_n$, which for the spin-1 chain corresponds to the effect of a random field along the z-axis [22, 53]. When dealing with the coupling to disorder, one has to bear in mind that the bosonized expression of the boson field is a series which contains higher-order harmonics [54] in the field $\phi_{1,2}$ from which the boson number operator can be written as

$$b_n^\dagger b_n = \sum_{m=1}^{\infty} A_m \cos(m\sqrt{2}\phi_a - 2mk_F x)\cos(m\sqrt{2}\phi_o), \tag{8}$$

where $x = na$. The term of order one has been treated in [22] and it is relevant when $K_a + K_o < 3$, while higher-order terms have been neglected. When the second-order term is taken into account, $A_2 \cos(2\sqrt{2}\phi_a - 4k_F x)\cos(2\sqrt{2}\phi_o)$, and performing a perturbation theory in $\cos(2\sqrt{2}\phi_o)$ at first order, an effective coupling to disorder is generated with the form

$$H^z_{\text{eff}} = (\xi_{4k_F}(x)A_2 e^{i\sqrt{8}\phi_a} + \text{h.c.}), \tag{9}$$

where $\xi_{4k_F}(x)$ is a Gaussian random variable with $\overline{\xi_{4k_F}(x)\xi^\star_{4k_F}(x')} = D_{\text{eff}}\delta(x - x')$. A renormalization group treatment of such a term gives

$$\frac{dD_{\text{eff}}}{dl} = (3 - 4K_a)D_{\text{eff}}, \tag{10}$$

and D_{eff} is relevant when $K_a < 3/4$. The terms with $m > 2$ in equation (8) become relevant for lower values of $K_a < 3/m^2$. Thus, along the critical line $g_1^\star = 0$ one expects a stable Luttinger liquid line up to $K_a^\star = 3/4$, and below it a Bose-glass phase between the Mott-insulating and Haldane-insulating phase takes place.

Let us note that even in a model where only the $m = 1$ term is kept in the expansion (8), the term (9) will be generated [53] by integrating over the fluctuations of the field θ_o. So the condition of stability $K^\star > 3/4$ is a generic one. As a consequence of this analysis, we expect that the HI–MI transition point in the presence of disorder has a 'Y' shape for $K_a > 3/4$ and a 'V' shape for $K_a < 3/4$. The phase diagrams presented in figure 1 focus on both cases, where for $U/t = 5$ we have $K_a = 0.6$ and hence we expect a 'V' case, while for $U/t = 3$ we have $K_a = 0.8$, which corresponds to a 'Y' case. Within the error bars, the data shown in figure 1 are compatible with those pictures.

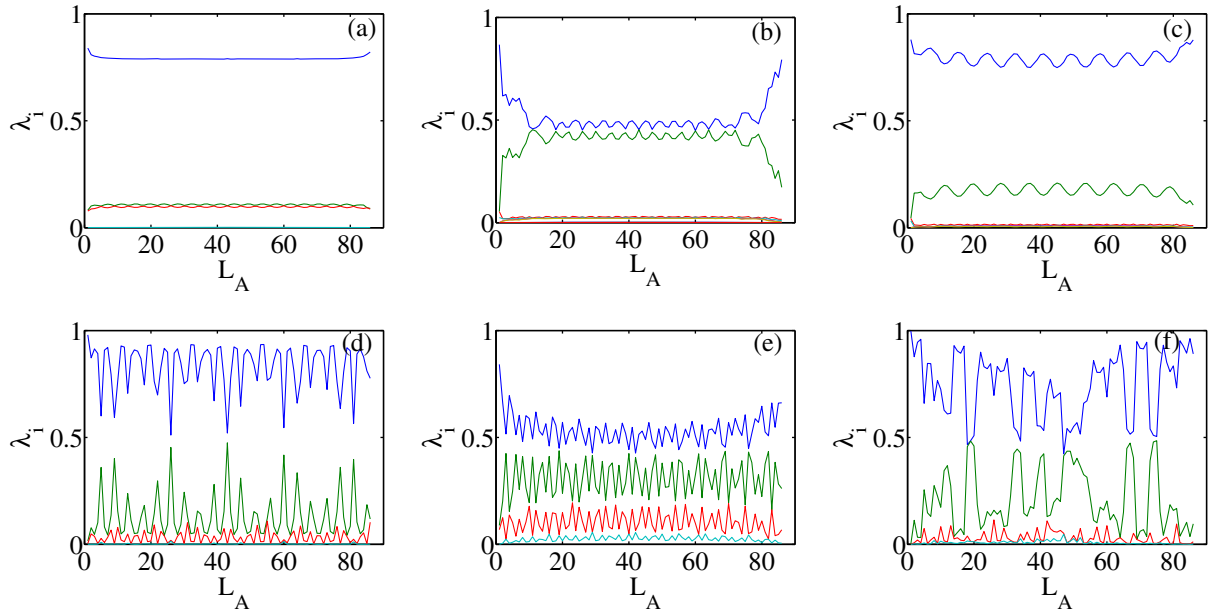

Figure 3. Entanglement spectrum of the extended Bose–Hubbard model under a quasiperiodic potential: largest eigenvalues as a function of the partition along the chain corresponding to (a) MI at $V/t = 0.5$ $\Delta/t = 0.2$; (b) HI, at $V/t = 3.3$, $\Delta/t = 0.2$; (c) DW, at $V/t = 3.6$, $\Delta/t = 0.2$; (d) ICDW, at $V/t = 1$ $\Delta/t = 6$; (e) SF, at $V/t = 0.5$, $\Delta/t = 3$ and (f) BG, at $V/t = 2$, $\Delta/t = 7.8$.

4. Entanglement spectra

The calculation of the entanglement spectrum is a novel approach to identify the quantum phases in several models. It is particularly useful to bring insight into topological phases and phases with non-local order parameter [55–58] and has been specifically analysed for the case of the Bose–Hubbard model [37, 59, 60]. The entanglement spectrum is defined as the spectrum $-\ln \lambda_i(L_A)$ of the effective Hamiltonian $-\ln \rho_A$, obtained by partitioning the system density matrix into two parts A and B (of length $L_A + L_B = L$) and tracing over the B part. It has been shown that the behaviour of the eigenvalues $\lambda_i(L_A)$ and their degeneracy differs in the various phases of the clean extended Bose–Hubbard model [37], thus allowing us to infer the structure of the phase diagram. We show here how the study of the entanglement spectrum can also give useful information in the disordered and aperiodic case.

In order to obtain the phase diagram, we take the combination of the first four largest eigenvalues $\zeta = \lambda_1^T - \lambda_2^T + \lambda_3^T - \lambda_4^T$, where $\lambda_i^T = (1/L)\sum_{L_A=1}^{L} \lambda_i(L_A)$. The result is illustrated in figure 2. The alternating regions of small and large values of ζ have a very good correspondence with the phases predicted from the study of correlation functions. This is explained in the study of the behaviour of the largest eigenvalues $\lambda_i(L_A)$ in the various phases, of which some examples are given in figure 3. In the MI phase in the clean case a degeneracy is found between λ_2^T and λ_3^T, as well as between λ_4^T and λ_5^T while λ_1^T is non-degenerate. This feature is also found to persist in the quasiperiodic case and yields a large value for ζ. In the SF phase, in contrast, the largest eigenvalues are almost equidistant; hence yielding a small ζ. In the clean case, the HI phase is characterized by a double degeneracy of the largest eigenvalues,

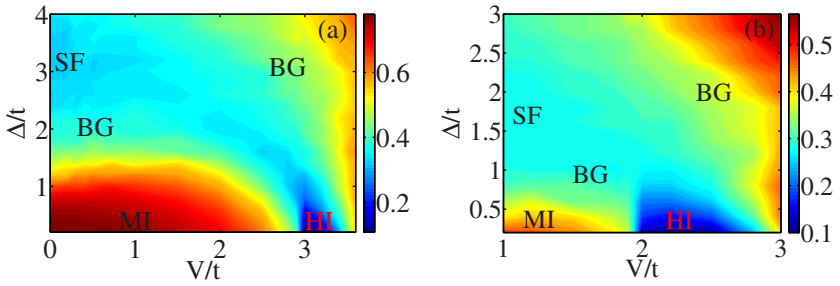

Figure 4. Phase diagram of the uniform disorder case from the entanglement spectrum function ζ defined in the text, (a) at $U/t = 5$, (b) at $U/t = 3$. Calculations performed with $L = 89$ and averaging over 30 disorder realizations. The various phases as found from the study of correlation functions are indicated.

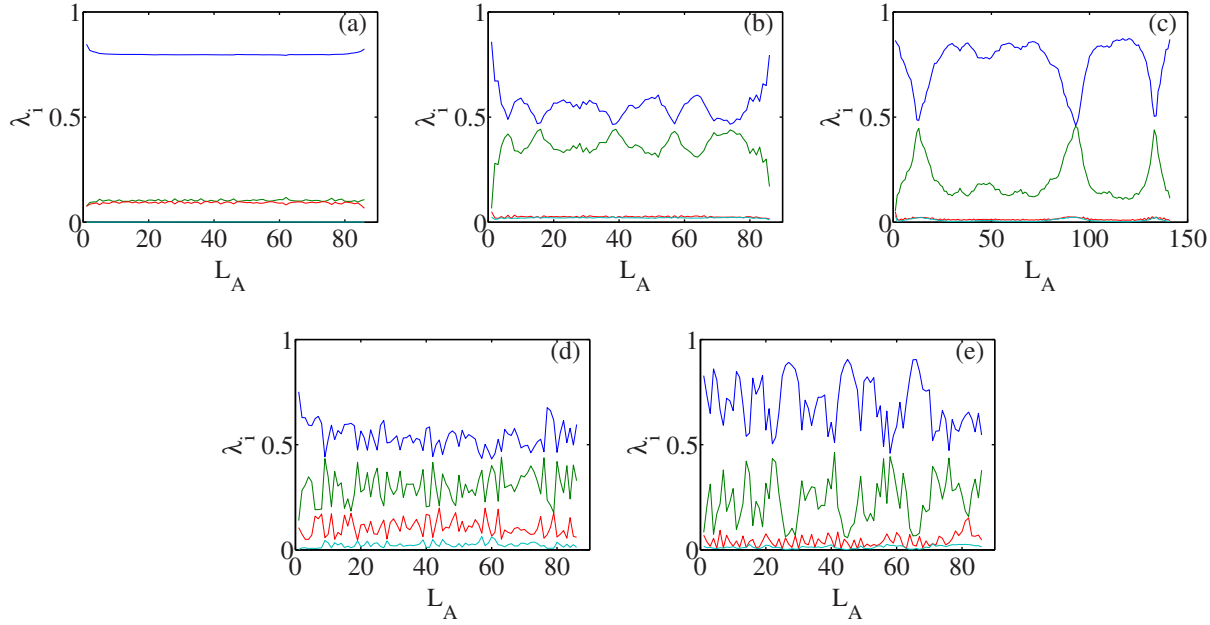

Figure 5. Entanglement spectrum of the extended Bose–Hubbard model in a single realization of the uniform random disorder: largest eigenvalues as a function of the partition along the chain corresponding to (a) MI at $V/t = 0.5$, $\Delta/t = 0.2$; (b) HI at $V/t = 3.3$, $\Delta/t = 0.2$; (c) BG (remnant of DW) at $V/t = 3.6$, $\Delta/t = 0.2$; (d) SF $V/t = 0$, $\Delta/t = 3.2$ and (e) BG at $V/t = 3.1$, $\Delta/t = 2$. The onsite interaction is $U/t = 5$ and $L = 89$.

implying another region of vanishing ζ.[7] Such degeneracy is gradually broken by increasing the strength of the quasiperiodic potential. In the DW phase no degeneracy is found in the clean case, thus allowing us to clearly distinguish this phase from the neighbouring HI; in the presence of a quasiperiodic potential, this phase gradually disappears. A similar level structure

[7] Since the simulation in figure 2(b) is done at integer filling the edge states cannot be eliminated, hence a small breaking of the double degeneracy is found at vanishing disorder, as in [31].

is found for the incommensurate DW. Finally, the BG phase displays a structure close to the ICDW phase, with a few large non-degenerate eigenvalues.

Next we consider the case of a uniform disorder. In figure 4 we show the phase diagram obtained from the entanglement spectrum. Some examples of the largest eigenvalues in the various phases are given in figure 5 for a given disorder realization. The main features are the same as in the quasiperiodic case: a unique large eigenvalue for the MI case and a few equally spaced eigenvalues for the SF case, the BG being intermediate between the above two configurations. We notice that although the DW disappears under finite-size scaling, some remnants of this phase are still visible in the eigenvalues at very low disorder strength.

5. Conclusions and perspectives

In conclusion, we have studied the phase diagram of one-dimensional polar bosons described by the extended Bose–Hubbard model in the presence of a uniform disorder or a quasiperiodic potential which acts as a pseudo-disorder. The phase diagram is numerically obtained from DMRG both by the analysis of correlation functions together with gap scaling, and by the study of the entanglement spectrum of the system. While the former method identifies precisely the transition lines, the study of the entanglement spectrum provides an independent check of the nature and location of the various phases, thus demonstrating itself to be a useful tool for exploring the various phases of correlated lattice bosons.

The phase diagrams obtained in the two cases are very different, due to the different nature of the (pseudo) disorder. In the case of a quasiperiodic potential we find four insulating phases (MI, HI, DW and incommensurate DW) and a SF phase, in addition to the Bose-glass phase. In the case of uniform disorder only two insulating phases remain (MI, HI), together with the SF and the Bose glass. In the latter case we focus on the boundary of the Haldane to Mott insulator phases at weak disorder. This is studied analytically using a bosonization and renormalization group approach. We predict that the shape of the phase diagram at the transition point depends on the strength of the on-site interactions, which can be either a 'Y' shape at weaker interactions or 'V' shape at stronger interactions. A scaling analysis of the DMRG data close to the transition point is consistent with these predictions.

It would be interesting to further explore the nature of the various phase boundaries [61, 62], as well as to understand how disorder affects the dynamical response in the various phases [63], extending the work done in the case of the Bose–Hubbard model.

Acknowledgments

We thank T Vekua for useful discussions. XD and LS are supported by the German Research Foundation (SA1031/6), the German-Israeli Foundation, and the Cluster of Excellence QUEST. EO and AM acknowledge support from the CNRS PEPS-PTI project 'Strong correlations and disorder in ultracold quantum gases', and AM from the Handy-Q ERC project no. 258608.

References

[1] Bloch I, Dalibard J and Zwerger W 2008 *Rev. Mod. Phys.* **80** 885
[2] Bloch I, Dalibard J and Nascimbene S 2012 *Nature Phys.* **8** 267
[3] Schneider U *et al* 2008 *Science* **322** 1520

[4] Jordens R *et al* 2008 *Nature* **455** 204
[5] Endres M *et al* 2012 *Nature* **487** 454
[6] Giamarchi T and Schulz H J 1988 *Phys. Rev.* B **37** 325
[7] Fisher M P A *et al* 1989 *Phys. Rev.* B **40** 546
[8] Roati G *et al* 2008 *Nature* **453** 895
[9] Billy J *et al* 2008 *Nature* **453** 891
[10] Kondov S S, McGehee W R, Zirbel J J and DeMarco B 2011 *Science* **334** 66
[11] Jendrzejewski F *et al* 2012 *Nature Phys.* **8** 398
[12] Fallani L *et al* 2007 *Phys. Rev. Lett.* **98** 130404
[13] Ospelkaus S *et al* 2010 *Science* **327** 853
[14] Griesmaier A *et al* 2005 *Phys. Rev. Lett.* **94** 160401
[15] Lu M *et al* 2011 *Phys. Rev. Lett.* **107** 190401
[16] Dalla E G, Torre Berg E and Altman E 2006 *Phys. Rev. Lett.* **97** 260401
[17] Berg E *et al* 2008 *Phys. Rev.* B **77** 245119
[18] Hyman Kun Yang R A, Bhatt R N and Girvin S M 1996 *Phys. Rev. Lett.* **76** 839
[19] Kun Yang Hyman R A, Bhatt R N and Girvin S M 1996 *J. Appl. Phys.* **79** 5096
[20] Monthus C, Golinelli O and Jolicoeur Th 1997 *Phys. Rev. Lett.* **79** 3254
[21] Monthus C, Golinelli O and Jolicoeur Th 1998 *Phys. Rev.* B **58** 805
[22] Brunel V and Jolicoeur Th 1998 *Phys. Rev.* B **58** 8481
[23] Saguia A, Boechat B and Continentino M A 2002 *Phys. Rev. Lett.* **89** 117202
[24] Damle K 2002 *Phys. Rev.* B **66** 104425
[25] Hida K 1999 *Phys. Rev. Lett.* **83** 3297
[26] Pai V and Pandit R 2005 *Phys. Rev.* B **71** 104508
[27] Mishra T *et al* 2009 *Phys. Rev.* A **80** 043614
[28] Dhar A *et al* 2011 *Phys. Rev.* A **83** 053621
[29] Imry Y and Ma S 1975 *Phys. Rev. Lett.* **35** 1399
[30] Shankar R 1990 *Int. J. Mod. Phys.* B **4** 2371
[31] Deng X, Citro R, Orignac E, Minguzzi A and Santos L 2012 arXiv:1203.0505
[32] White S R 1992 *Phys. Rev. Lett.* **69** 2863
White S R 1993 *Phys. Rev.* B **48** 10345
[33] Schollwoeck U 2005 *Rev. Mod. Phys.* **77** 259
[34] Schollwoeck U 2011 *Ann. Phys., NY* **326** 96
[35] Noack R M and Manmana S 2005 *AIP Conf. Proc.* **789** 93
[36] Hallberg K 2006 *Adv. Phys.* **55** 477
[37] Deng X and Santos L 2011 *Phys. Rev.* B **84** 085138
[38] Affleck I, Kennedy T, Lieb E H and Tasaki H 1987 *Phys. Rev. Lett.* **59** 799
[39] Giamarchi T and Schulz H J 1987 *Europhys. Lett.* **3** 1287
[40] Rapsch S, Schollwöck U and Zwerger W 1999 *Europhys. Lett.* **46** 559
[41] Prokof'ev N V and Svistunov B V 1998 *Phys. Rev. Lett.* **80** 4355
[42] Degli Esposti Boschi C, Ercolessi E, Ortolani F and Roncaglia M 2003 *Eur. Phys. J.* B **35** 465
[43] Cazalilla M A 2004 *J. Phys. B: At. Mol. Opt. Phys.* **37** S1
[44] Roscilde T 2008 *Phys. Rev.* A **76** 063605
[45] Roux G, Barthel T, McCulloch I P, Kollath C, Schollwöck U and Giamarchi T 2008 *Phys. Rev.* A **78** 023628
[46] Albert M and Leboeuf P 2010 *Phys. Rev.* A **81** 013614
[47] Timonen J and Luther A 1985 *J. Phys. C: Solid State Phys.* **18** 1439
[48] Schulz H J 1986 *Phys. Rev.* B **34** 6372
[49] Chen W, Hida K and Sanctuary B C 2003 *Phys. Rev.* B **67** 104401
[50] Degli Esposti Boschi C, Ercolessi E, Ortolani F and Roncaglia M 2003 *Eur. Phys. J.* B **35** 465
[51] Albuquerque A F, Hamer C J and Oitmaa J 2009 *Phys. Rev.* B **79** 054412

[52] Hu S, Normand B, Wang X and Yu L 2011 *Phys. Rev.* B **84** 220402
[53] Orignac E and Giamarchi T 1998 *Phys. Rev.* B **57** 5812
[54] Haldane F D M 1981 *Phys. Rev. Lett.* **47** 1840
[55] Li H and Haldane F D M 2008 *Phys. Rev. Lett.* **101** 010504
[56] Calabrese P and Lefevre A 2008 *Phys. Rev.* A **78** 032329
[57] Regnault N, Bernevig B A and Haldane F D M 2009 *Phys. Rev. Lett.* **103** 016801
[58] Lauchli A M, Bergholtz E J, Suorsa J and Haque M 2010 *Phys. Rev. Lett.* **104** 156404
[59] Alba V, Haque M and Laeuchli A M 2012 *Phys. Rev. Lett.* **108** 227201
[60] Alba V, Haque M and Laeuchli A M 2012 arXiv:1212.5634
[61] Altman E, Kafri Y, Polkovnikov A and Refael G 2010 *Phys. Rev.* B **81** 174528
[62] Ristivojevic Z, Petkovìc A, Le Doussal P and Giamarchi T 2012 *Phys. Rev. Lett.* **109** 026402
[63] Roux G, Minguzzi A and Roscilde T 2013 arXiv:1302.2404